Supporting Information

Layer-by-Layer Assembly of Magnetic-Core Dual Quantum Dot-Shell Nanocomposites for Fluorescent Lateral Flow Detection of Bacteria

Chongwen Wang[a,b,d,#], Wanzhu Shen[b,c,#], Zhen Rong[b,#], Xiaoxian Liu[a], Bing Gu[d,e,*], Rui Xiao[a,b,*], Shengqi Wang[a,b,c,*]

[a] *College of Life Sciences, Anhui Agricultural University, Hefei 230036, PR China.*
[b] *Beijing Key Laboratory of New Molecular Diagnosis Technologies for Infectious Disease, Beijing Institute of Radiation Medicine, Beijing 100850, PR China.*
[c] *Anhui Medical University, Hefei 410073, PR China.*
[d] *Xuzhou Medical University, Xuzhou 221004, PR China.*
[e] *Department of Laboratory Medicine, Affiliated Hospital of Xuzhou Medical University, Xuzhou 221004, PR China.*

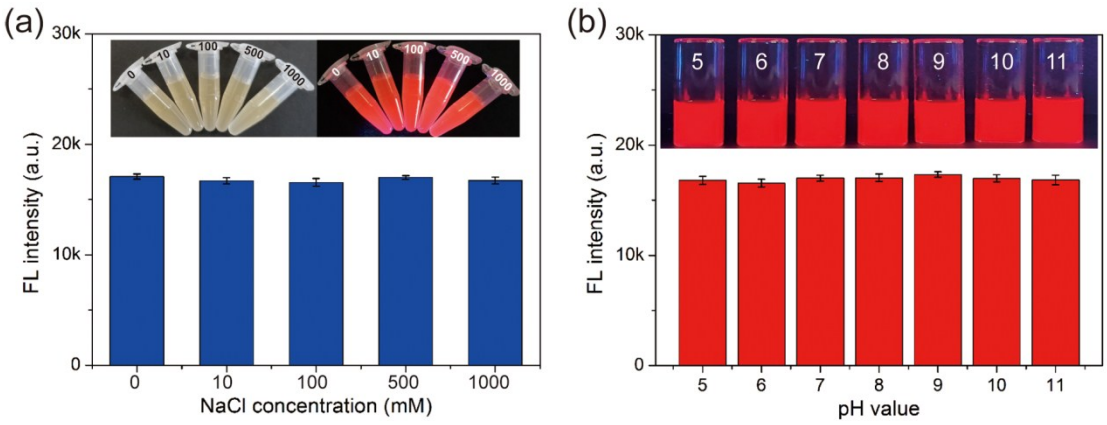

Fig. S1 (a) Stability of Fe_3O_4@DQDs in various salt concentrations. (0 mM–1000 mM NaCl). (b) Fluorescence intensities of Fe_3O_4@DQDs at different pH values.

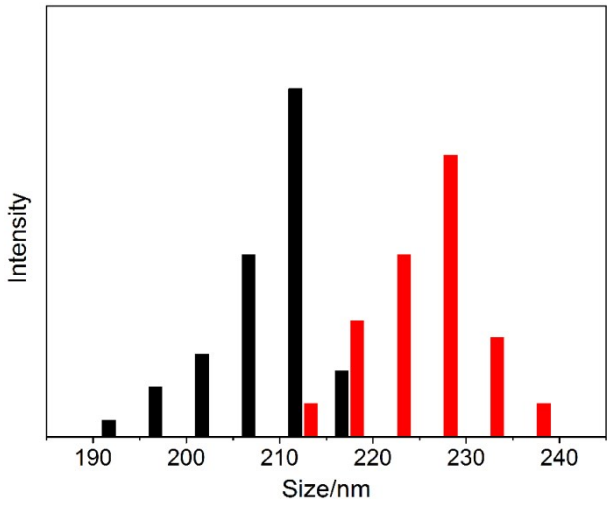

Fig. S2 DLS distributions of Fe_3O_4@DQDs (black) and antibody-conjugated Fe_3O_4@DQDs (red).

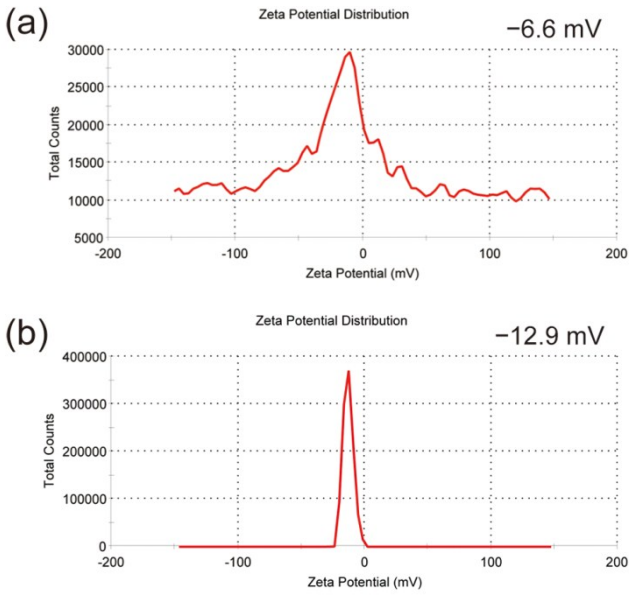

Fig. S3 Zeta potential of Fe_3O_4@DQDs (a) and antibody-conjugated Fe_3O_4@DQDs (b) in deionized water.

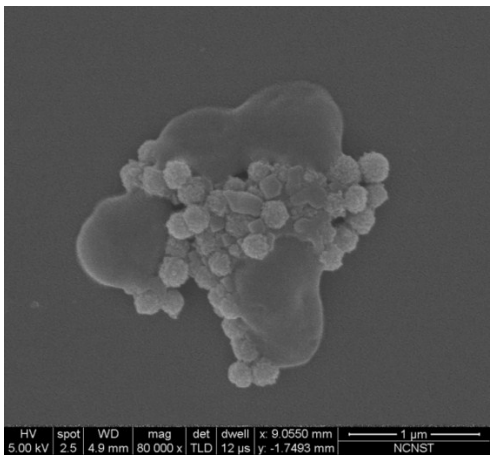

Fig. S4 SEM image of the formed Fe_3O_4@DQD–*S. pneu*moniae immunocomplexes.

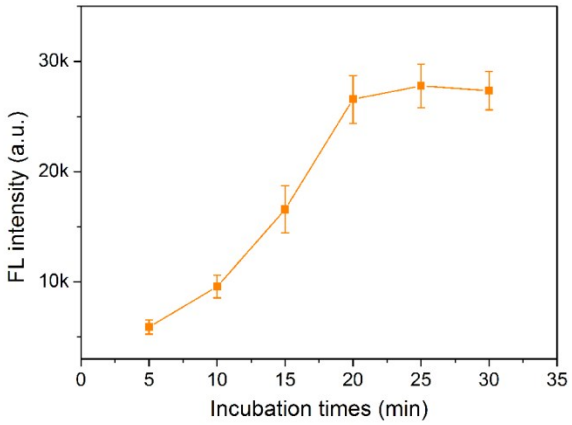

Fig. S5 Effects of immuno-Fe_3O_4@DQDs incubation time on the T line for the LFA detection system.

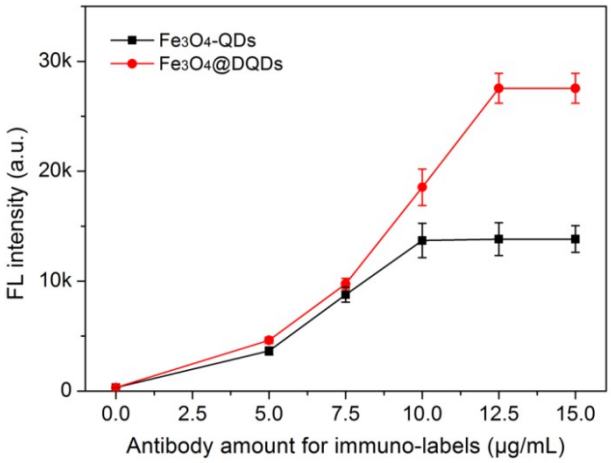

Fig. S6 Fluorescence intensity of the test line versus the amount of *S. pneumoniae* antibody modified on the Fe_3O_4@DQDs. The error bars represent the standard deviations from three measurements.

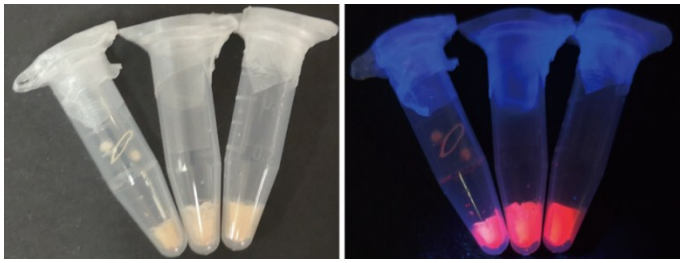

Fig. S7 Photographs of freeze-dried immuno-Fe_3O_4@DQDs under visible (left) and UV light (right).

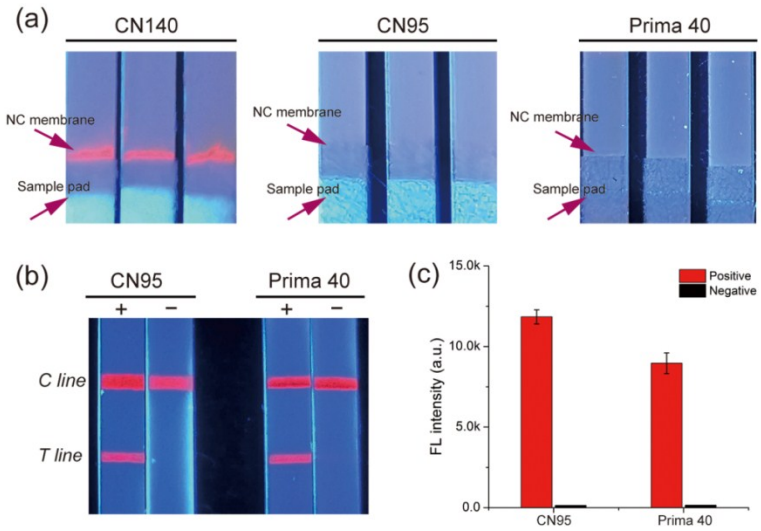

Fig. S8 Optimization of NC membranes on the the LFA strip. (a) Effects of the three different NC membranes employed in the LFA strip. (b) Images and (c) fluorescence intensity of the test LFA strips using CN95 and Prima 40 membranes. Error bars represent the standard deviations calculated from the three separate experiments.

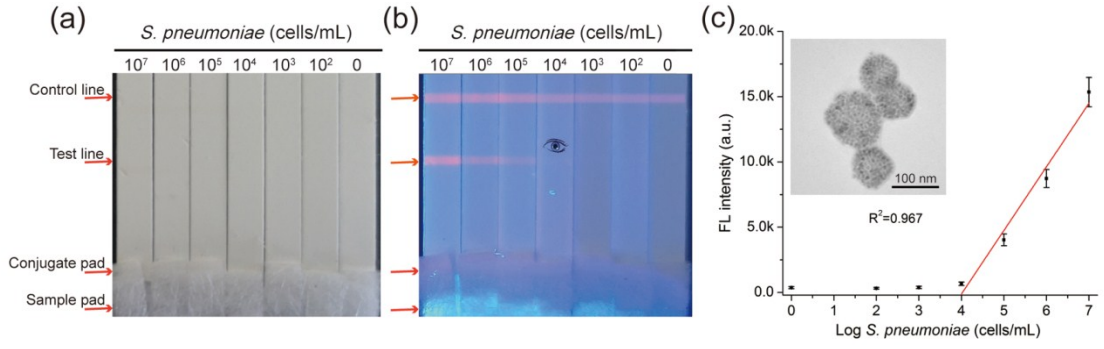

Fig. S9 Analytical performance of commercial QD microsphere-based fluorescent LFA strip. (a) Photographs and (b) fluorescence pictures of QD microsphere-based LFA strip for *S. pneumoniae* detection. (c) Calibration curve for *S. pneumoniae* at a concentration range of 10^4-10^7 cells/mL. The inset shows the TEM image of commercial QD microspheres.

Table S1. Recovery rates of *S. pneumoniae* spiked in two kind biological samples and detected by the proposed assay.

Sample	Spiked (cells/mL)	Detected (cells/mL)	Recovery (%)	RSD (%)
Blood	2×10^6	1.90×10^6	95.0	5.82
	2×10^4	1.83×10^4	91.5	7.47
	20	16.3	81.5	9.73
Sputum	2×10^6	1.96×10^6	98.0	3.50
	2×10^4	1.87×10^4	93.5	5.46
	20	19.2	96.0	8.14

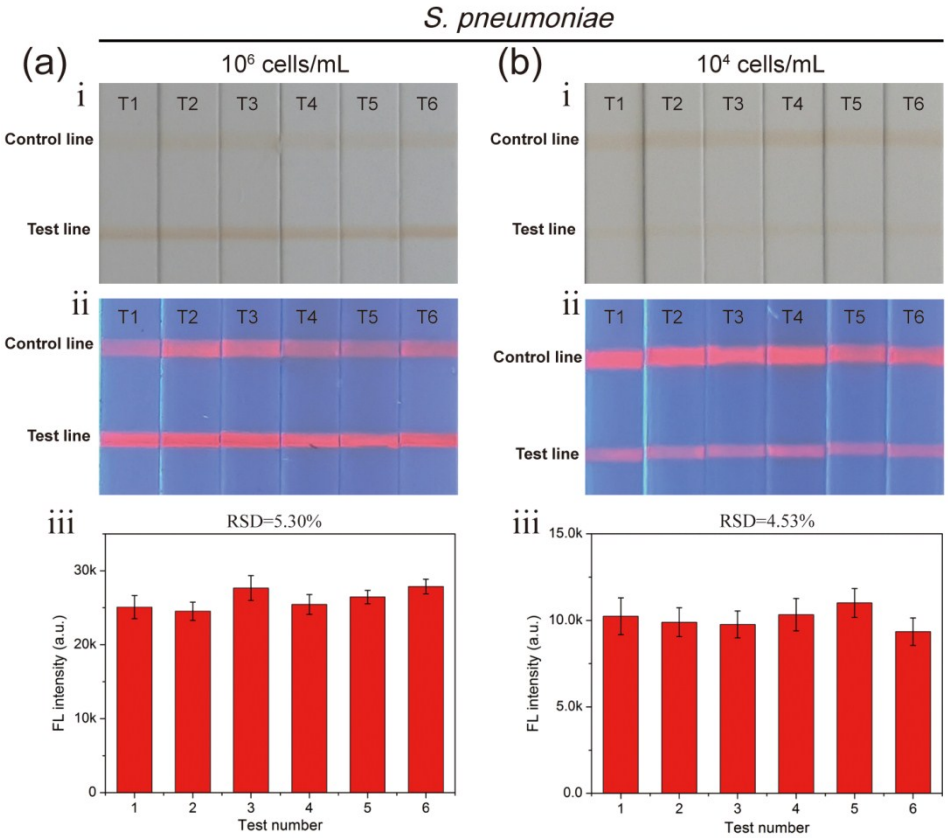

Fig. S10 Assay reproducibility of six batches of *S. pneumoniae* at a concentration of 10^6 cells/mL (a) and 10^4 cells/mL (b) in human whole blood. The error bars represent the standard deviations from three separate experiments.